Environmental Science and Pollution Research (2022) 29:41053–41064
https://doi.org/10.1007/s11356-021-18066-1

RESEARCH ARTICLE

Abelmoschus esculentus (Okra) seed extract for stabilization of the biosynthesized TiO_2 photocatalyst used for degradation of stable organic substance in water

Mohammad Aslam[1] · Ahmad Zuhairi Abdullah[1] · Mohd Rafatullah[2] · Ahmad Fawad[3]

Received: 3 August 2021 / Accepted: 8 December 2021 / Published online: 27 January 2022

Abstract

The seed extract of *Abelmoschus esculentus* (AE), also known as *Okra*, was used as a source of reducing and capping agents to synthesized biogenic titanium dioxide nanoparticles (TiO_2 NPs) due to its rich flavonoid contents. The synthesized AE-TiO_2 nanoparticles were further evaluated by the effect of loading of TiO_2 NPs and irradiation time on the photocatalytic degradation of methylene blue dye. The synthesized TiO_2 NPs were then characterized by scanning electron microscopy (SEM), X-ray diffraction (XRD), thermogravimetric analysis (TGA), energy dispersive X-ray spectroscopy (EDS), Fourier transformed infrared (FTIR) spectroscopy, Raman spectra, UV–visible spectrophotometry, and particle size distribution (PSD). The findings confirmed the successful synthesis of the spherical anatase phase of TiO_2 NPs, as well as the existence of phytochemicals in the extract, which were involved in the capping/stabilization of NPs. The synthesized TiO_2 NPs were found to be 60–120 nm in size and almost uniformly distributed throughout the sample. The photocatalytic activity measured in a 300 mL cylindrical photochemical reactor and irradiated with 250 watts UV lamp was investigated based on methylene blue degradation. Effects of irradiation time and catalyst loading were elucidated and correlated with the characteristics of the catalysts. The findings revealed that the synthesized TiO_2 NPs were well-dispersed, stable, and could achieve more than 80 % degradation in 240 min of irradiation with 90 mg/L of AE-TiO_2 NPs loading compared to only 70 % by the commercial one. These results suggested that AE-TiO_2 NPs possesses significant catalytic activity, and the photocatalytic process could be used to degrade, decolorize, and mineralize the methylene blue dye. The polyphenolic tannins present in the extract were the reason behind the desirable characteristics of the nanoparticles and better photocatalytic activity of AE-TiO_2 NPs.

Keywords Titanium dioxide · Nanoparticles · Green synthesis · *Abelmoschus esculentus* · Photocatalyst · Methylene blue

Introduction

In recent years, there has been incredible attention in nanoparticle research. Nanobiotechnology is a technology that enriches the use of materials of nanometer dimensions in various areas of science such as nanomaterials, biotechnology, material science, physics, and chemistry. Nanobiotechnology also facilitates the improvement of good hygiene, reliable and environmentally fusion, and collection of metal nanoparticles, along with various chemical and physical methods for synthesis of metal and metal oxide nanoparticles (Barkalina et al. 2014). Recently, nanoparticle biosynthesis has gained serious attention owing to the increasing need for non-toxic chemicals, antibacterial, antiviral, diagnostic, anticancer, targeted drug delivery of eco-friendly solvents, and renewable resources (Gebre and Sendeku 2019). Conventional methods such as solvothermal, sol-gel, direct precipitation, hydrothermal, co-precipitation, sonothermal, and microwave methods are time-consuming and require specialized instrumentation (Anupama et al. 2018). Moreover, they often use harmful solvents or reagents as costly substrates along with potentially harmful impacts (Anupama

Responsible Editor: Sami Rtimi

✉ Ahmad Zuhairi Abdullah
chzuhairi@usm.my

[1] School of Chemical Engineering, Engineering Campus, Universiti Sains Malaysia, 14700 Nibong Tebal, Penang, Malaysia

[2] School of Industrial Technology, Universiti Sains Malaysia, 11800 USM Penang, Malaysia

[3] Department of Applied Chemistry, Aligarh Muslim University, Aligarh 202002, India

et al. 2019). Additionally, the chemically synthesized nanoparticles are described as less stable with high agglomeration tendency (Abdullah et al. 2009; Saxena et al. 2012). Henceforth, natural and biological materials can be used as an alternative source to solve these issues.

Scientists have reported various approaches to synthesize metal and metal oxide nanoparticles by using different biological sources such as plant extracts, bacteria, fungi, algae, and yeast (Ahmad et al. 2020; Santhoshkumar et al. 2014). The biosynthesized nanoparticles are environmentally benign, economical, energy efficient, and facile synthesis method which is sufficiently reliable for large-scale industrial production (Nabi et al. 2020). The plant intermediation biosynthesis of nanoparticles has become one of the significant parts of nanobiotechnology research in the world today. The synthesis of nanoparticles by chemical techniques can result in certain toxic species being developed on the surface of nanoparticles (Ahmad et al. 2020; Kuppusamy et al. 2016). To overcome this problem, a "green chemistry" approach based on the synthesis of metal nanoparticles using plants and plant extracts can be a highly efficient and effective approach because they can contribute certain reducing/stabilizing agents such as terpenoids, alkaloids, phenolic compounds, enzymes, flavonoids, proteins, and polysaccharides to facilitate the formation of more biocompatible nanoparticles (Nabi et al. 2020; Mohamed et al. 2018). The use of plant extracts is said to be more effective in comparison to biological processes as it eliminates the challenging conditions of storage of cell culture environment which are extremely difficult to accomplish (Makarov et al. 2014). Moreover, plants and crops have long been thought to be useful and inexpensive sources for biological nanoparticles production (Narayanan and Sakthivel 2011). Consequently, researchers used plant extracts to find new low-cost pathways for the synthesis of nanoparticles (Mohanpuria et al. 2008).

Photocatalytic removal of organic pollutants has appeared as one of the excellent methodologies for the treatment of harmful organic effluents, which uses semiconductors as catalysts such as ZnO, TiO_2, ZnS, WO_3, CdS, and Fe_2O_3 (Rajabi et al. 2013). The interest has grown substantially among researchers towards heterogeneous photocatalyst after the first revolutionary paper in the 1970s by Paola et al. (2012). The benefits of photocatalytic activities over conventional methods, including rapid oxidation, no creation of polycyclic compounds, complete oxidation of contaminant, and highly efficient, have been demonstrated by Saien et al. (2011). As a result, the use of heterogeneous photocatalysts emerges as a viable option for organic effluent treatment, and the catalyst reduced to a nano size can exhibit distinct features compared to their properties at the macroscale, allowing for photocatalytic removal of organic pollutants (Rajabi et al. 2013).

Titanium dioxide (TiO_2) nanoparticles have been widely used as an environmentally friendly and clean photocatalyst in recent years. TiO_2 material is an important semiconducting transition metal oxide with unique properties such as ease of control, low cost, and non-toxic (Santhoshkumar et al. 2014). It also possesses good resistance to chemical erosion, making it suitable for solar cells, chemical sensors, and environmental applications (Khan et al. 2002). The electrical, magnetic, and optical properties of these nanoparticles are better compared to those of their bulk counterparts (Xu et al. 2008). TiO_2 exists in both amorphous and crystalline forms, with the most common crystalline polymorphous of anatase, rutile, and brookite (Mahshid et al. 2007).

In addition to waste reduction, reaction procedural simplification, and process intensification, the green features of any catalytic or biocatalytic process can also be evaluated based on the synthesis procedure of the catalysts involved in those processes (Zinatizadeh et al. 2007). In this context, very few preliminary works on rare metal nanoparticles such as lanthanum and titanium have been reported in previous studies through greener synthesis routes. Several research groups synthesized TiO_2 nanoparticles using natural products from various plants such as *Mentha arvensis* (Waseem et al. 2020), *Lemon* peel (Ghulam et al. 2020), *Psidium guajava* (Santhoshkumar et al. 2014), *Ocimum americanum* (Vijayakumar et al. 2020), *Ageratina alttissima* L (Ganesan et al. 2016), *Vitex negundo* (Ambika and Sundrarajan 2016), *Curcuma longa* (Jalill et al. 2016), *Vigna unguiculate* (Chatterjee et al. 2017), and *Moringa oleifera* (Patidar and Jain 2017). The biocompatible and non-toxic properties of TiO_2 NPs generally make them suitable for use in biomedical research including bone tissue engineering as well as in pharmaceutical industries. Therefore, there is a need to establish new approaches for the production of TiO_2 NPs. The productions of several metals, their oxides, their nitrides, their sulfides, and their carbides are seen as more sustainable processes. There is an urgent need for such approaches to produce materials that are biologically safe, environmentally friendly, and cost-effective in order to reduce or prevent expensive and eco-destructive methodologies in the synthetic industries. As a result, new methods for synthesizing TiO_2 nanoparticles can be improved.

Abelmoschus esculentus (Okra) that belongs to the mallow family is an important vegetable that can be found in almost every country in the world and is generally used in traditional medicine. The main inorganic elements in this plant are K, Na, Mg, and Ca, and it has antibacterial, antioxidant, and antispasmodic properties (Duan et al. 2015). Organically, Okra seed is specifically composed of oligomeric catechins, flavonol derivatives, total phenol, vitamins, and polyphenols (Duan et al. 2015). The polyphenolic content of Okra confers antioxidant activity (Jochebed et al. 2017). According to a previous study, the results of Okra

seeds FTIR showed that proteins, fats, and amino acids were responsible for the major spectra bands of the samples and the protein hydrolysates exhibited greater antioxidant properties (Nnamezie et al. 2021). Moreover, various spectra bands of functional groups such as amino acids, alkane compound, enzymatic protein hydrolysates, methoxy methyl ether compound, and carboxylic acids were found in Okra seeds. The plant extract of Okra has been used for the biosynthesis of various metal and metal oxide nanoparticles (Anupama et al. 2019; Nitin et al. 2021; Elmusa et al. 2021) with encouraging results. However, seed extract of Okra has yet to be investigated for TiO_2 NPs. It is hypothesized that the same nanoparticle formation mechanism reported for the other metals or metal oxides can also work in the desired way in the case of TiO_2 nanoparticles. Thus, the novelty of the current study lies in the fact that the biosynthesized TiO_2 NPs using *Abelmoschus esculentus* (Okra) seed extract is reported here for the first time, along with their impressive photocatalytic activity. The seeds are known to be a rich source of biomolecules such as phenols and polyphenolic tannins which might act as reducing/capping agents during the synthesis of TiO_2 NPs (Elmusa et al. 2021). The optical and photocatalytic properties of the synthesized TiO_2 NPs were also investigated and benchmarked against commercial TiO_2.

Materials and methods

Materials

All the materials were used as received without further purification. Titanium hydroxide (metatitanic acid, TiO_3H_2 purity>97%), methylene blue ($C_{16}H_{18}ClN_3S$), ethanol ((C_2H_6O), purity 99.9%), nitric acid (HNO_3, 68%), hydrochloric acid (HCl, 38%), and sodium hydroxide (NaOH, ≥96.0%) were purchased from Sigma Aldrich (Germany). The green synthesis of TiO_2 NPs was carried out by using the aqueous seed extract of Okra. These seeds were purchased from a local market outside the Universiti Sains Malaysia campus. Distilled water and the filter papers having pore size of 1.2 µm (Whatman, England) were used during the preparation of the seed extract. For comparison of results, a commercial anatase TiO_2 from Aldrich (USA) was also used in the photocatalytic activity study.

Preparation of Abelmoschus esculentus (AE) seed extract

The typical *Abelmoschus esculentus* (Okra) seeds are as shown in Fig. 1. The seeds were first washed with distilled water several times. Around 10 g of seeds was then weighed and grained using mortar and pestle. The crushed seeds were

Fig. 1 *Abelmoschus esculentus* (Okra) seeds

dispersed in 250 mL of distilled water and heated for 4 h at 90°C for the extraction process. Then, the solution was filtered using a Whatman No. 1 filter paper (Surya et al. 2018).

Synthesis of TiO_2 nanoparticles

Two hundred fifty milliliters of Okra seed extract was added dropwise to 0.5 M of titanium hydroxide solution on constant stirring for 4 h at 60 °C for the synthesis of TiO_2 NPs until the pH reached 8. The solution was then centrifuged at 4000 rpm for 10 min and the precipitate was separated and washed with ethanol to remove any ionic and other soluble impurities. Next, the synthesized NPs were dried in an oven for 24 h at 80 °C. The dried NPs were then crushed with the help of mortar and pestle. Finally, the fine powder TiO_2 synthesized with the assistance of Okra extract (AE-TiO_2 NPs) was achieved after the calcination at 500 °C for 2.5 h in a muffle furnace (Ghulam et al. 2020).

Characterization of TiO_2 NPs

FTIR measurements were taken using a Bruker vertex 70 system. Powdered and dried TiO_2 NPs and AE-TiO_2 NPs were pelleted with potassium bromide (KBr) (1:3 ratio). The spectra were recorded in the wavenumber range from 400 to 4000 cm^{-1}. XRD analysis was conducted at D8 Bruker Advance system in the 2θ range of 5–80° using Cu α radiation (k=1.540593 Å). The tool was equipped with a graphite monochromator and operated at a current of 50 mA and a voltage of 40 kV. Thermogravimetric and differential thermal analyses (TGA-DTA) were performed in air within a temperature range from 28 to 800 °C and at a temperature rate of 20 °C min^{-1} using a Shimadzu DTG-60H system (Japan). Scanning electron microscopy (SEM) images of TiO_2 NPs and AE-TiO_2 NPs formed were taken

from JFM-6510 LV (JEOL, Japan). Meanwhile, the elemental composition of synthesized nanoparticles was studied using energy dispersive X-ray spectroscopy (EDS). Using an inVia Renishaw's Centrus 1C4A91 UK Raman spectroscopy system with a spectral resolution of 2 cm^{-1}, the UV Raman spectra of TiO_2 NPs were recorded. The laser line at 532 nm edge (power 0.1%) was used as an excitation source with grating 2400 l/mm (vis). The exposure time and spectral ranges are 40 s and 101.56 cm^{-1} to 1002.41 cm^{-1} (center—1111 cm^{-1}), respectively. The UV–vis absorption spectra of the TiO_2NPs and AE-TiO_2NPs were recorded at room temperature employing a PerkinElmer Lambda 45 UV–visible spectrophotometer. The samples were scanned from 200 to 900 nm with a resolution of 1 nm and a scan speed of 960 nm/min (Vijayakumar et al. 2020).

Photocatalytic behavior

Methylene blue (MB) was chosen as a model organic substance to demonstrate and compare the photocatalytic activity of the AE-TiO_2NPs. A 300 mL photochemical reactor made from a cylindrical glass and equipped with 250 watts of UV lamp, a central QVR jacketed tube, and a 250 watts power controller fuse box along with a circular water system was used to make the setup. The photocatalytic reactor used in the experiment is shown in Fig. 2. Different catalyst loadings (15–90 mg) were first dispersed in 100 mL of distilled water and mixed with 30 mg/L of MB at a pH of 10 under continuous stirring of 30 min in dark condition to achieve adsorption and desorption. The experiment under UV lamp was then carried out from 0 to 240 min with 10 mL of sample aliquots taken every 20 min. Then, the degraded amount of MB was checked using a UV–vis spectrophotometer at maximum absorption peak of 664 nm. The standard calibration curve was prepared by plotting between the recorded absorbances and the concentrations of methylene blue solution in the range of 0–50 mg/L. The following equation is used to calculate the photodegradation efficiency of the photocatalyst.

$$\text{Dye degradation}(\%) = \frac{C_o - C_t}{C_o} \times 100\% \quad (1)$$

where C_o is the initial concentration while C_t is the concentration at time t of MB (Fardood et al. 2020).

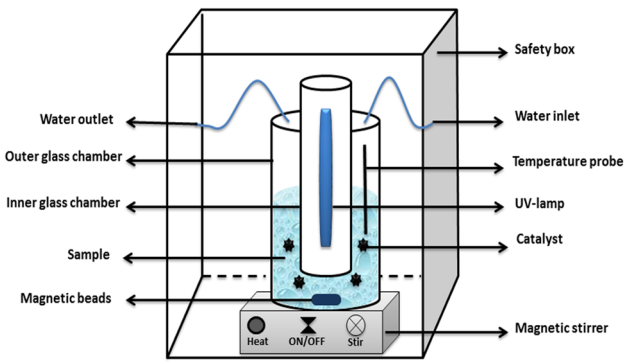

Fig. 2 Photocatalytic reactor used in this study

Results and discussion

Characterization of TiO_2 nanoparticles

The X-ray diffraction (XRD) patterns of TiO_2 NPs and AE-TiO_2 NPs are shown in Fig. 3. The sharpness of the peak indicates the crystalline nature of both types of TiO_2 NPs to deny any detrimental effect posed by the extract on the crystallinity. The characteristic peaks of TiO_2 NPs and AE-TiO_2 NPs at 2θ are 25.31°, 36.80°, 37.87°, 38.91°, 48.10°, 53.91°, 55.10°, 62.71°, 68.78°, and 70.31° and 25.28°, 36.93°, 37.77°, 38.55°, 48.03°, 53.88°, 55.74°, 62.64°, 68.74°, and 70.28°, respectively. The miller indices (*hkl*) peaks for both NPs are (110), (101), (004), (112), (200), (105), (211), (204), (220), and (107). The pattern of synthesized AE-TiO_2 NPs is quite similar to the reference pattern (JCPDS Card No.: 01-073-1764). However, the occurrence of the most intense peak is visibly shifted slightly from 28.31° to 25.28° to indicate slightly regular crystallites of the AE-TiO_2 NPs. The average nanoparticle size of the synthesized NPs is calculated using the Debye-Scherrer formula (Moradnia et al. 2020).

$$D = \frac{K\lambda}{\beta \cos\theta} \quad (2)$$

where λ denotes the wavelength of X-ray ($\lambda = 1.541874$ Å), K is the Scherrer constant (k= 0.9), β is the full width at half maximum (FWHM), D represents particle size, and 2θ is the angle of X-ray diffraction peak.

The average crystallite size of TiO_2 NPs and AE-TiO_2 NPs were estimated to be 35.42 and 37.73 nm, respectively. The distinct peaks of X-ray confirmed the anatase phase of both types of TiO_2 NPs. All peaks were attributed to the facets of the crystalline TiO_2 NPs tetragonal anatase phase. However, any other peaks associated with the impurity were not observed to indicate the complete removal of crystalline materials during the photocatalyst preparation procedures. The sharp peaks indicate that the TiO_2 NPs were of high crystallinity, which was considered to be beneficial for photocatalytic activity and was directly associated with the charge recombination rate. The high crystallinity reduces the number of trapped electrons, which serve as recombination centers for photo-induced electron hole pairs (Carneiro et al.

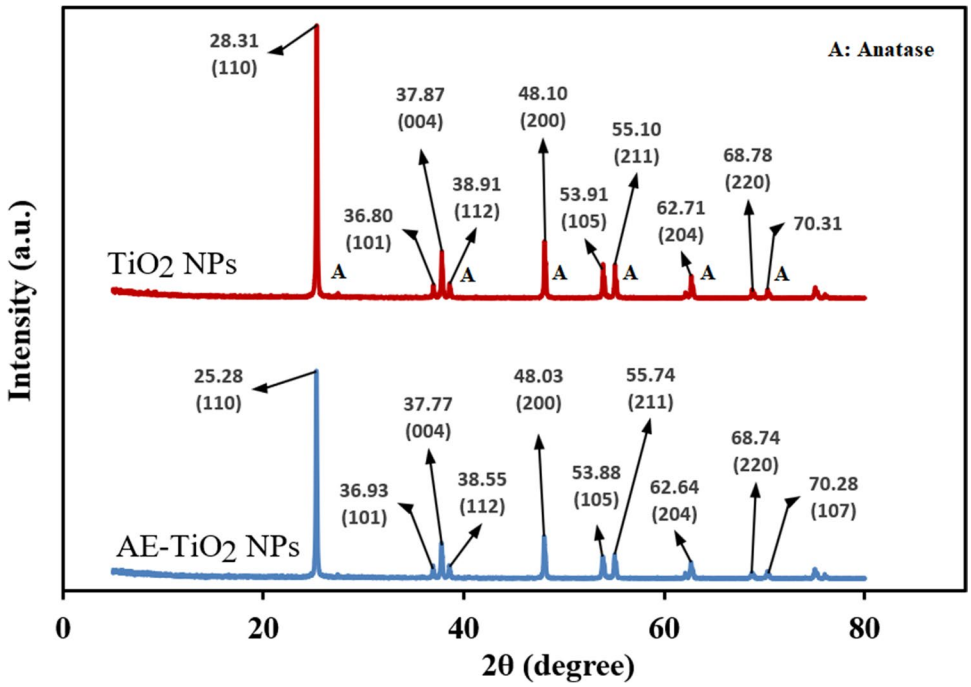

Fig. 3 XRD patterns of commercial TiO_2 NPs and AE-TiO_2 NPs

2011). Furthermore, the significantly long-life span of the electron hole pairs corresponding to the high charge separation considerably produces a large number of electrons and holes, thereby initiating the photocatalytic redox reactions. As a result, it was concluded that the AE-TiO_2NPs prepared were mainly of anatase phase and small sized which could be due to the surfactant behavior of the Okra extract.

In addition, the FTIR spectroscopy method was used to identify potential biomolecules based on chemical groups in the Okra seed extract that were responsible for the capping/reduction of precursor metal ions that played a significant role in synthesizing NPs. The FTIR spectrum of the extract is shown in Fig. 4a. A broad and intense band at 3448 cm^{-1} indicates the presence of hydroxyl groups, which could be due to the presence of phenolic substances in the extract (Moradnia et al. 2020). The presence of phenolic substances was most likely due to the existence of polyphenolic tannins, which might have capped the surface of TiO_2 nanoparticles in the synthesis of AE-TiO_2 NPs. The peak intensity at 1648 cm^{-1} and 2150 cm^{-1} points to the presence of C=O anhydrides from the carbonyl group with stretching vibrational frequency. Finally, a broad peak at 678 cm^{-1} indicates the presence of C-H flexion, to conclude that aromatic compounds were also present in the extract.

The typical FTIR spectra of TiO_2 NPs and AE-TiO_2 NPs recorded in the range of 500 cm^{-1} to 4000 cm^{-1} absorption band are shown in Fig. 4b. Broad peaks recorded at 3438 cm^{-1} and 3424 cm^{-1} and small peaks at 1642 cm^{-1} and 1630 cm^{-1} could be related to the existence of the hydroxyl group and surface adsorbed water, respectively (Ghaly et al. 2011). The hydroxyl group could play a significant role in

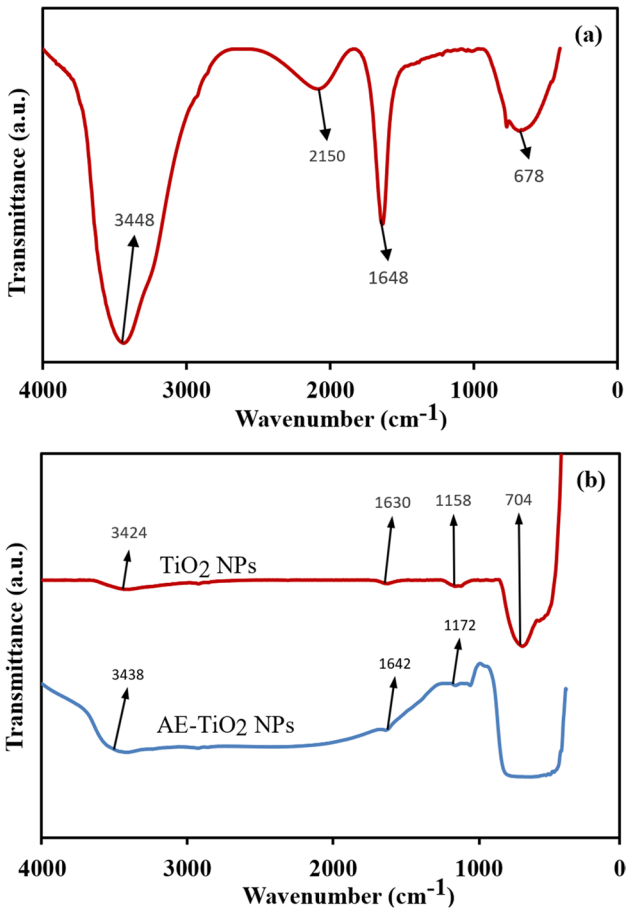

Fig. 4 FTIR spectra of **a** seed extract of Okra and **b** TiO_2 NPs and AE-TiO_2 NPs

improving photocatalytic activity by improving the interaction with the aqueous solution during the reaction. The enhanced hydroxyl group presence on the surface of TiO_2 NPs was responsible for increased electron transportability and, as a result, an increase in photocatalytic activity was expected (Carneiro et al. 2011). Based on the intensity of the peaks, AE-TiO_2 NPs could be concluded to be relatively more hydrophilic. The small peaks at 500–700 cm^{-1} are associated with the Ti-O stretching and Ti-O-Ti bridging stretching modes (Peiro et al. 2011). The absorption peak at 704 cm^{-1} could reveal the contribution of the AE-TiO_2 NPs in the anatase phase as previously reported (Karakitsou and Verykios 1993).

Thermogravimetric analysis was performed on the calcined AE-TiO_2 NP powder. The thermogravimetric analysis (TGA) and thermal differential analysis (TDA) profiles are depicted in Fig. 5. The TGA curve represents the weight loss of the AE-TiO_2 NPs, while the DTA curve represents the energy gains or losses during the process. Initially, the dehydration of any entrapped water molecules observed as an endothermic effect was noticed below 100 °C, resulting in a minimal weight loss observed. A noticeable exothermic peak in the DTA curve could be ascribed to the evaporation of carbonized residues on the surface of the AE-TiO_2 NPs. No significant weight loss was observed after 500 °C, suggesting the thermal stability of the AE-TiO_2 NP powder. Similar findings have also been reported (Ramimoghadam et al. 2014).

Scanning electron microscopy (SEM) images were used to analyze the form, morphology, and the size of the synthesized nanoparticles. Fig. 6a and b show that the AE-TiO_2 NPs had rather spherical shapes, whereas TiO_2 NPs had sphere-like surface morphology, respectively. It is also visible that AE-TiO_2 NPs managed to maintain the individuality of the crystallites compared to the commercial TiO_2 NPs. However, clear voids were created between the

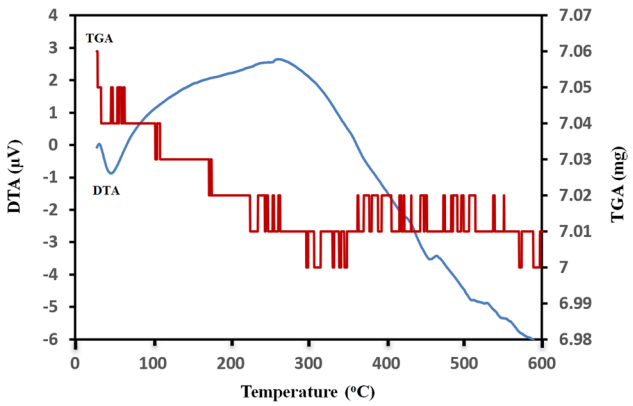

Fig. 5 Thermogravimetric analysis (TGA/DTA) results of the calcined AE-TiO_2 NPs

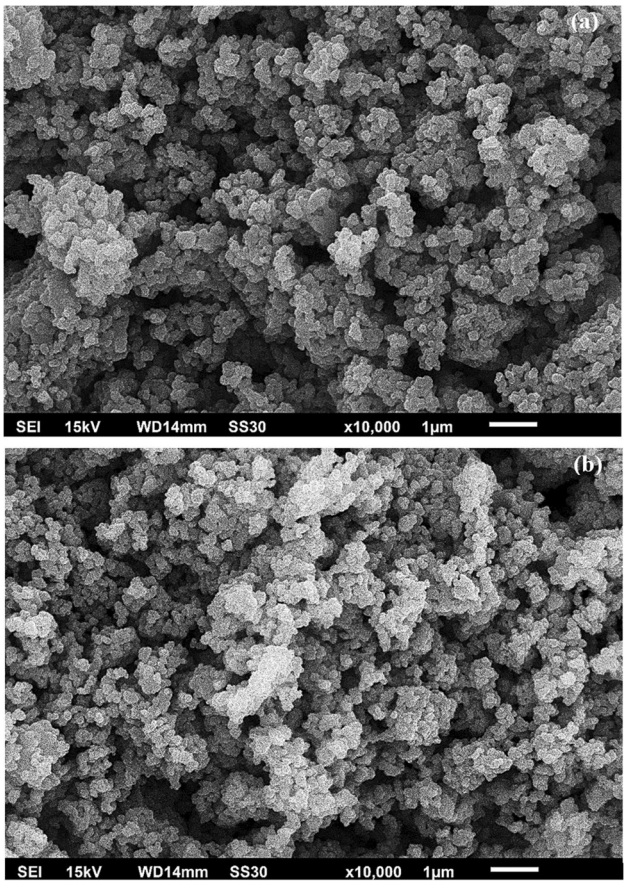

Fig. 6 SEM images of **a** AE-TiO_2 NPs and **b** TiO_2 NPs

crystallites in the case of AE-TiO_2 NPs. The particle sizes of AE-TiO_2 NPs and TiO_2 NPs were found to be in the size range of 80–120 nm. Based on the crystallite sizes as concluded based on the XRD results, only minimum agglomeration of the individual crystallites could be concluded, especially on the AE-TiO_2 NPs despite the calcination temperature of 500 °C for 2.5 h.

Fig. 7a and b show the histogram of the particle size distribution of nanoparticles which are calculated with the help of the ImageJ software. The peaks in the distribution occur in the size range of 100–120 nm and 120–140 nm for AE-TiO_2 NPs and TiO_2 NPs, respectively. A large number of small and distinct AE-TiO_2 NPs were spotted along with some larger agglomerated NPs, which are easily visible in the SEM images. The slight agglomeration of AE-TiO_2 NPs could be caused by the pH of the solution. Moreover, the biomolecules in the seed extract of *Abelmoschus esculentus* such as polyphenols, flavonoids, alkaloids, terpenoids, free amino acids, and tannins could play significant roles in enhancing dispersions between NPs by reducing their agglomeration during the synthesis (Alessandra et al. 2019) and thus could play a key role in reducing particle agglomeration. The individuality of the particles could ensure the

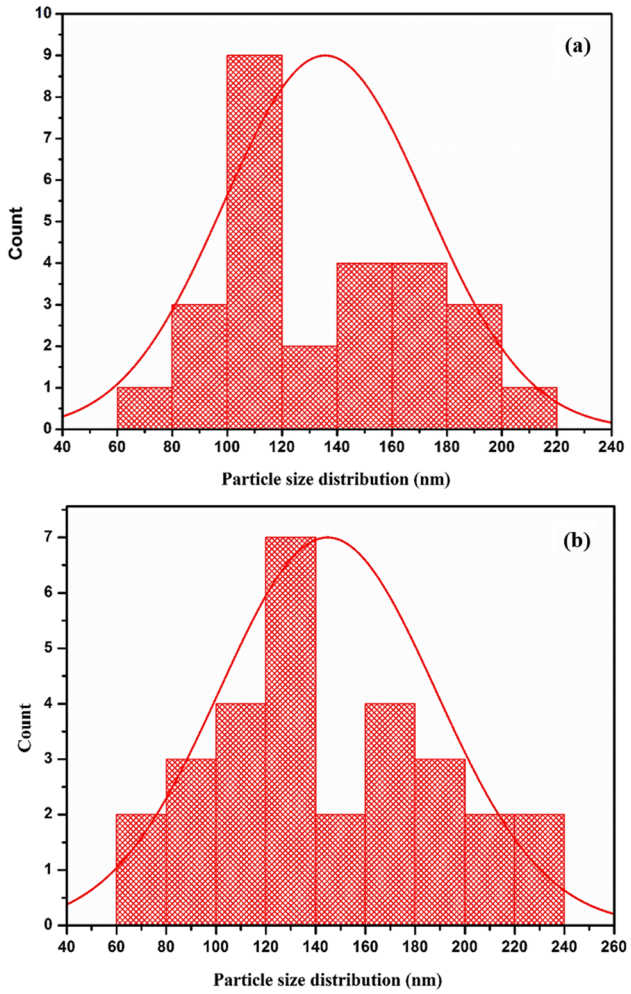

Fig. 7 Particle size distribution of **a** AE-TiO_2 NPs and **b** TiO_2 NPs

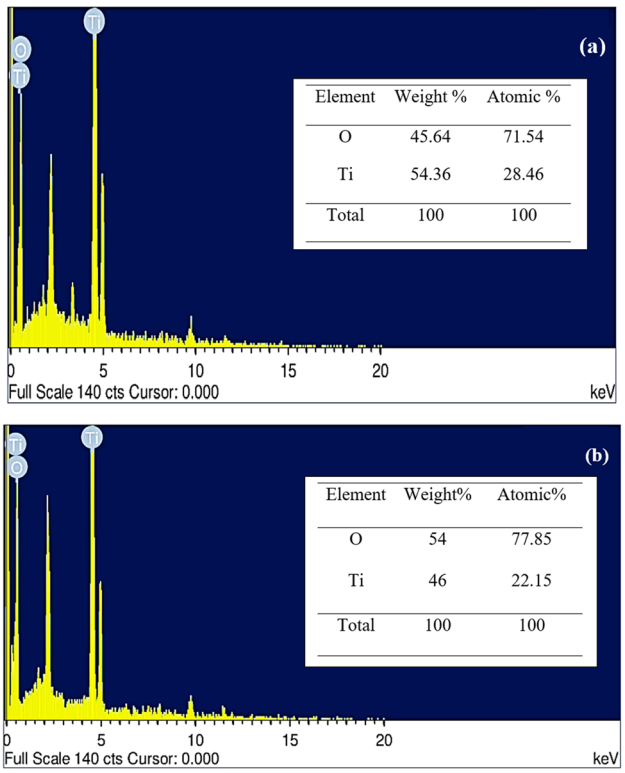

Fig. 8 EDS spectra and corresponding elemental compositions of **a** AE-TiO_2 NPs and **b** TiO_2 NPs

extra surface area for the interaction with the solution during the photocatalytic study.

Additionally, an energy dispersive X-ray spectroscopy (EDS) method was used to determine the elemental composition of NPs. The corresponding weight and atomic percentages of both the nanoparticles are shown in Fig. 8a and b. The occurrence of only titanium and oxygen peaks affirmed the synthesis of pure anatase AE-TiO_2 NPs. There seem to be no other impurity peaks found to indicate the complete burning of Okra extract during the calcination process. The results also pointed to the conclusion that as the Ti:O atomic ratios were not exactly 1:2 (1:2.5 and 1:3.5 for AE-TiO_2 NPs and TiO_2 NPs, respectively), other titanium oxide species besides TiO_2 could also exist in the two photocatalyst samples. In conclusion, the use of Okra extract in the synthesis of TiO_2 could cause the reduction of higher titanium oxide species.

UV–vis spectroscopy was used to examine the optical properties of the synthesized samples. The aqueous seed extract was found to have a peak at 256 nm, which was consistent with the published results (Sandhanasamy and Mohamad 2021) as shown in Fig. 9. The UV–vis spectrum of AE-TiO_2 NPs suggests that the higher absorption was recorded in the range of 250–400 nm. Changes in the crystalline phase and average crystalline size correspond to the sharp absorption peak. The synthesis of AE-TiO_2 NPs was confirmed by the sharp absorbance peak around 350–400

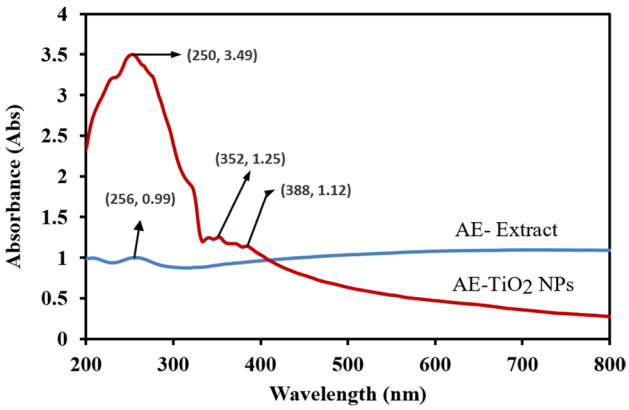

Fig. 9 UV–vis absorption spectra for *Abelmoschus esculentus* seed extract and AE-TiO_2 nanoparticles

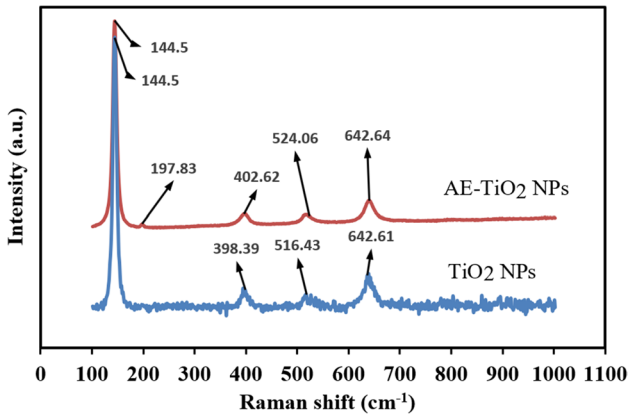

Fig. 10 Raman spectra of AE-TiO_2 NPs and TiO_2 NPs

nm. The strong absorption peaks at 352 and 388 nm which are observed within the range from 200 to 800 nm confirm the successful synthesis of metallic AE-TiO_2 NPs. As a result, the investigated nanomaterial was deemed highly suitable for catalytic applications (Fardood et al. 2020).

Further analysis of the TiO_2 NP structural phase was performed by Raman spectroscopy. As illustrated in Fig. 10, anatase generally has six Raman active modes of factor group analyzed which are indicated by peaks at 144 cm^{-1} (Eg), 197 cm^{-1} (Eg), 399 cm^{-1} (B_{1g}), 513 cm^{-1} (A_{1g}), 519 cm^{-1} (B_{1g}), and 639 cm^{-1} (Eg). Five active Raman modes of AE-TiO_2 NPs were observed for anatase phase which are 144.5 cm^{-1} (Eg), 197.83 cm^{-1} (Eg), 402.62 cm^{-1} (B_{1g}), 524.06 cm^{-1} (B_{1g}), and 642.64 cm^{-1} (Eg). Meanwhile, the TiO_2 NPs have only four active Raman modes which are 144.5 cm^{-1} (Eg), 398.39 cm^{-1} (B_{1g}), 516.43 cm^{-1} (B_{1g}), and 642.61 cm^{-1} (Eg). The Raman peaks at 144.5 and 197.83 cm^{-1} correspond to the presence of Ti Ti bonds in the octahedral chains. The Raman bands observed at 402.62, 524.06, and 642.64 cm^{-1} are generated from Ti O bonds. The basic characteristics of the Raman spectra of AE-TiO_2 NPs also bear a close resemblance to TiO_2 NPs, with a reduction in peak intensity. However, the decrease in the intensity peaks confirms the absorption of biomolecules in the seed extract of *Abelmoschus esculentus*.

Photocatalytic activity

The photocatalytic degradation of methylene blue (MB) was investigated using green synthesized TiO_2 (AE-TiO_2) NPs and commercial TiO_2 NPs by photocatalytic reactor under UV light irradiation. The results illustrated in Fig. 11 indicate that the AE-TiO_2 NPs could enhance the degradation efficiency of MB as compared to TiO_2 NPs. The AE-TiO_2 NPs achieved more than 80% photocatalytic activity, which was quite satisfactory when compared to TiO_2 NPs, which showed 70% removal. This could be attributed to the

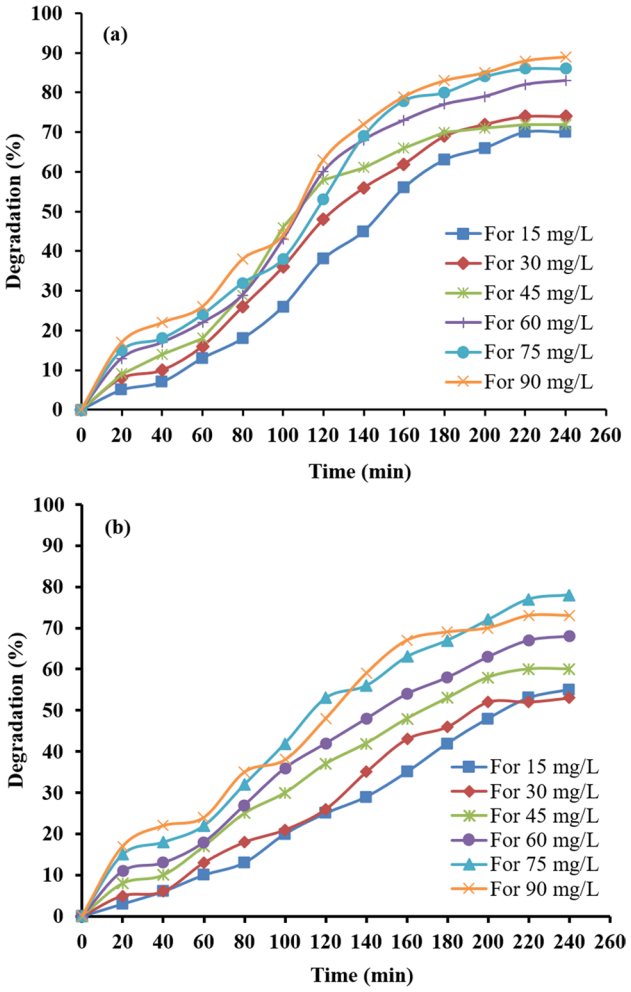

Fig. 11 Profiles of photocatalytic degradation of methylene blue with time for different catalyst loadings of **a** AE-TiO_2 NPs and **b** TiO_2 NPs

desirable morphology and exciting optical properties of TiO_2 NPs synthesized using the green synthesis technique. The time required for maximum dye degradation was approximately 200–240 min of exposure to irradiation. The degradations of dye with respect to time and concentration by the photocatalysts are observed in Fig. 11, which illustrates the gradual degradation of MB with respect to time.

Dye color degradation can occur as a consequence of the breakup of chromophores inside the dye molecule, which gives the dye its distinct color (Aravind et al. 2021). The decolorization efficiency increased with the increase in TiO_2 loading, particularly up to 90 mg/L. This is owing to the belief that TiO_2 enhances the active sites for dye adsorption on the surface of the photocatalyst including the generation of free hydroxyl radicals (•OH). However, increasing the catalyst loading (>90 mg/L) does not result to a significant increase in decolorization and degradation efficiency. This behavior could be caused by a variety of factors, including increased light scattering and screening effects, along with

possible photocatalyst particle agglomeration, which reduces the active catalytic surface. As a result, a TiO_2 loading of 90 g/L was considered the optimum value for the photocatalytic activities. The photocatalytic activity increased as the irradiation time was increased, and the increase in the concentration of catalyst also increased the degradation efficiency. Moreover, the presence of reducing organics such as polyphenolic tannins in Okra seed extract could be the reason for the improved MB degradation efficiency as compared to commercial TiO_2 NPs. It is known that when inorganic substances are heated with reducing substances in an oxidative environment during the calcination step, the organic reductant could reduce the oxidation ability of the inorganic species. In this study, this was observed as higher purity of TiO_2 in AE-TiO_2 NPs as compared to TiO_2 NPs. However, the complete chemical analysis of organic complex formation in biosynthesized TiO_2 NPs is very challenging due to the complex nature of interactions involved in the synthesis process leading to the formation of TiO_2 NPs. Therefore, further research needs to be undertaken in order to clearly understand the interaction between the titanium and phenolic groups during the synthesis process and their impact on photocatalytic activity. In this study, AE-TiO_2 NPs demonstrated higher photocatalytic activity compared to commercial TiO_2 NPs. This was associated with the smaller particle size and lower presence of higher oxidation species of titanium of the former. These were the beneficial effects of the use of Okra extract in its synthesis.

The mechanism of photocatalytic degradation is shown in Fig. 12. It is hypothesized that when AE-TiO_2 NPs were exposed to UV irradiation, more electrons were energized from the valence band (VB) to the conduction band (CB), resulting in the formation of more positively charged holes (by h^+) on the surface. Generally, a reaction takes place between electrons and holes present on the surface of the semiconductor, with electrons (e^-) capable of reducing O_2 to $O_2^{-\bullet}$, as well as positive holes (h^+) reacting with H_2O or OH^- to produce hydroxyl radicals ($^{\bullet}OH$) (Sabouri et al. 2020). These free radicals are strong oxidative species, which are capable to degrade harmful organic pollutants such as dye molecules and produce degradation products. When a positive hole reacts with a water molecule, it produces an $OH^{\bullet}$ radical and hydrogen ions (H^+). Additionally, a superoxide anion is produced by the reaction of an electron with oxygen, which leads to the formation of an $OH^{\bullet}$ radical through a series of reactions. Moreover, Both $H_2O^{\bullet}$ and $OH^{\bullet}$ radicals are powerful oxidizing agents that can quickly attack MB dye molecules, causing total mineralization and the formation of CO_2, NH_4^+, SO_3^{2-}, and H_2O. Irradiation time has a significant impact on MB dye degradation, decolorization, and mineralization, as the total organic carbon value decreased as the irradiation time increased. As a result, h^+ and $OH^{\bullet}$ are by far the most important active species for MB degradation by AE-TiO_2 NP photocatalyst throughout the reaction. The reactions involved during the photocatalytic degradation are expressed as follows (3–15) (Akbari et al. 2020):

$$\text{Catalyst} + \text{Irradiation} \rightarrow h^+_{VB} + e^-_{CB} \tag{3}$$

$$TiO_2 + h\nu(UV) \rightarrow TiO_2^* + h^+ + e^- \tag{4}$$

$$TiO_2\left(h^+\right) + H_2O \rightarrow TiO_2 + H^+ + OH^{\bullet} \tag{5}$$

$$TiO_2(e^-) + O_2 \rightarrow TiO_2 + O_2^{-\bullet} \tag{6}$$

$$MB + hv \rightarrow MB^* \tag{7}$$

$$TiO_2 + MB^* \rightarrow MB^{*\bullet} + TiO_2(e^-) \tag{8}$$

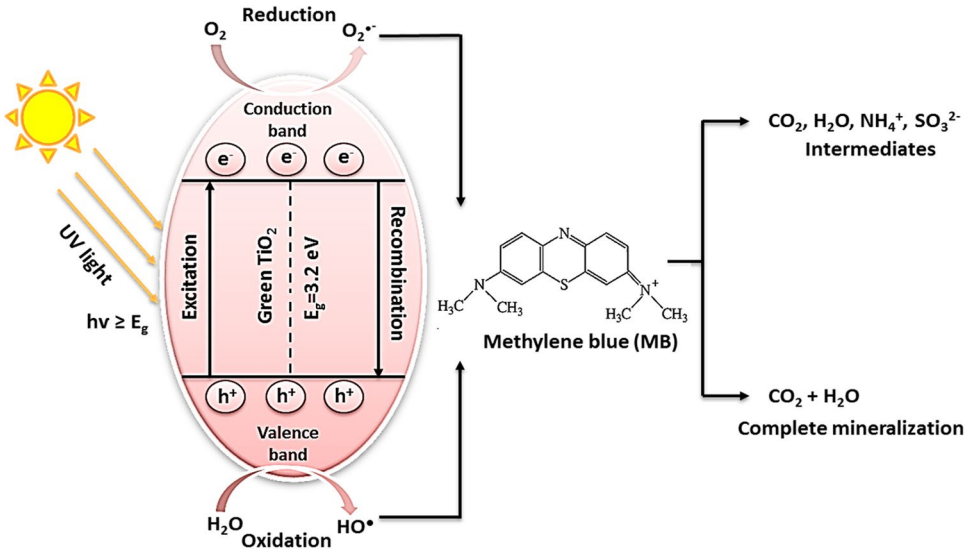

Fig. 12 Mechanism of methylene blue photocatalytic degradation by AE-TiO_2 NPs

$$TiO_2(e^-) + O_2 \rightarrow O_2^{\bullet -} + TiO_2 \quad (9)$$

$$O_2^{\bullet -} + H^+ \rightarrow HO_2^{\bullet} \quad (10)$$

$$HO_2^{\bullet} + H^+ + e^- \rightarrow H_2O_2 \quad (11)$$

$$H_2O_2 + e^- \rightarrow OH^- + OH^{\bullet}$$
$$MB^{+\bullet} + OH^{\bullet}\left(\text{or}O_2^{\bullet -}\text{or}HO_2^{\bullet}\right) \rightarrow\rightarrow \text{Reduced products} \quad (12)$$

$$2TiO_2 + hv \rightarrow TiO_2(e^-) + TiO_2(H^+) \quad (13)$$

$$TiO_2\left(H^+\right) + MB \rightarrow MB^{+\bullet} + TiO_2 \quad (14)$$

$$TiO_2\left(H^+\right) + H_2O \rightarrow OH^{\bullet} + H^+ + TiO_2$$
$$MB + OH^{\bullet} \rightarrow\rightarrow \text{Mineralization products} \quad (15)$$

Conclusions

TiO_2 NPs were successfully synthesized biogenically from *Abelmoschus esculentus* (Okra) seed extract without the use of any additional solvents, catalysts, or templates. The presence of various biomolecules such as phenols and tannins in seed extract was responsible for the reduction of metallic ions and acts as capping/reducing agents during the green synthesis of TiO_2 NPs, thus stabilizing the NPs. The synthesized TiO_2 NP particle sizes occurred in the range of 60–120 nm and of spherical anatase crystals. The EDS plot shows that the particles were of high purity and free of contamination. When compared to commercial TiO_2 NPs, green synthesized TiO_2 NPs possess higher methylene blue degradation efficiency of 89 % in 240 min of irradiation with 90 mg/L loading of catalyst. Nanoparticles with a high surface-to-volume ratio might have more active adsorption sites, which in turn enhanced the photocatalytic activity. The outstanding photocatalytic activity of green synthesized TiO_2 NPs showed that the formed photocatalyst could potentially be effectively used for water purification. The stability and reusability of catalyst also demonstrated that these photocatalysts have the potential to address the limitations of the photocatalytic process.

Author contribution Mohammad Aslam planned and carried out the experimental work conceptualized by Ahmad Zuhairi Abdullah who is also involved in securing the research funding. Mohd Rafatullah contributed to the analysis and interpretation of results and drafting of the manuscript. Ahmad Fawad contributed by providing some critical resources needed for the study while at the same time involved in data interpretation.

Funding The authors acknowledge the Long-Term Research Grant Scheme (LRGS) from the Ministry of Higher Education of Malaysia (LRGS/1/2018/USM/01/1/3).

Data availability Not applicable.

Declarations

Ethics approval and consent to participate Not applicable.

Consent for publication Not applicable.

Competing interests Not applicable.

References

Abdullah AZ, Razali N, Lee KT (2009) Optimization of K/SBA-15 catalyzed transesterification of palm oil using response surface methodology. Fuel Process Technol 90:958–964. https://doi.org/10.1016/j.fuproc.2009.03.023

Ahmad W, Jaiswal KK, Soni S (2020) Green synthesis of titanium dioxide (TiO_2) nanoparticles by using *Mentha arvensis* leaves extract and its antimicrobial properties. Inorg Nano-Metal Chem 50(10):1032–1038. https://doi.org/10.1080/24701556.2020.1732419

Akbari A, Sabouri Z, Hosseini HA, Hashemzadeh A, Khatami M, Darroudi M (2020) Effect of nickel oxide nanoparticles as a photocatalyst in dyes degradation and evaluation of effective parameters in their removal from aqueous environments. Inorg Chem Commun 115:107867. https://doi.org/10.1016/j.inoche.2020.107867

Alessandra D, Massimo L, Ettore N, Eliana BS, Patricia D, Antonello S (2019) Abelmoschus esculentus (L.): Bioactive components' beneficial properties focused on antidiabetic role for sustainable health applications. Molecules 24:38. https://doi.org/10.3390/molecules24010038

Ambika S, Sundrarajan M (2016) [EMIM] BF 4 ionic liquid-mediated synthesis of TiO_2 nanoparticles using *Vitex negundo Linn* extract and its antibacterial activity. J Mol Liq 221:986–992. https://doi.org/10.1016/j.molliq.2016.06.079

Anupama C, Kaphle A, Udayabhanu Nagaraju G (2018) *Aegle marmelos* assisted facile combustion synthesis of multifunctional ZnO nanoparticles: study of their photoluminescence, photo catalytic and antimicrobial activities. J Mater Sci Mater Electron 29:4238–4249. https://doi.org/10.1007/s10854-017-8369-1

Anupama RP, Julia G, Shamsheera KO, Abraham J (2019) Bio-inspired green synthesis of zinc oxide nanoparticles using *Abelmoschus esculentus* mucilage and selective degradation of cationic dye pollutants. J Phys Chem Solids 127:265–274. https://doi.org/10.1016/j.jpcs.2019.01.003

Aravind M, Amalanathan M, Mary MSM (2021) Synthesis of TiO_2 nanoparticles by chemical and green synthesis methods and their multifaceted properties. SN Appl Sci 3:409. https://doi.org/10.1007/s42452-021-04281-5

Barkalina N, Charalambous C, Jones C, Coward K (2014) Nanotechnology in reproductive medicine: emerging applications of nanomaterials. Nanomed Nanotechnol Biol Med 10:921–938. https://doi.org/10.1016/j.nano.2014.01.001

Carneiro JT, Savenije TJ, Moulijn JA, Mul G (2011) How phase composition influences optoelectronic and photocatalytic properties of TiO_2. J Phys Chem C 115:2211–2217. https://doi.org/10.1021/jp110190a

Chatterjee A, Ajantha M, Talekar A, Revathy N, Abraham J (2017) Biosynthesis, antimicrobial and cytotoxic effects of titanium dioxide nanoparticles using *Vigna unguiculata* seeds. Mater Lett 9:95–99. https://doi.org/10.25258/ijpapr.v9i1.8047

Duan H, Wang D, Li Y (2015) Green chemistry for nanoparticle synthesis. Chem Soc Rev 44:5778–5792. https://doi.org/10.1039/C4CS00363B

Elmusa F, Aygun A, Gulbagca F, Seyrankaya A, Göl F, Yenikaya C, Sen F (2021) Investigation of the antibacterial properties of silver nanoparticles synthesized using *Abelmoschus esculentus* extract and their ceramic applications. Int J Environ Sci Technol 18:849–860. https://doi.org/10.1007/s13762-020-02883-x

Fardood ST, Forootan R, Moradnia F, Afshari Z, Ramazani A (2020) Green synthesis, characterization, and photocatalytic activity of cobalt chromite spinel nanoparticles. Mater Res Express 7:015086. https://doi.org/10.1088/2053-1591/ab6c8d

Ganesan S, Babu IG, Mahendran D, Arulselvi PI, Elangovan N, Geetha N, Venkatachalam P (2016) Green engineering of titanium dioxide nanoparticles using Ageratina altissima (L.) King and HE Robines. Medicinal plant aqueous leaf extracts for enhanced photocatalytic activity. Ann Phytomed 5:69–74. https://doi.org/10.21276/ap.2016.5.2.8

Gebre SH, Sendeku MG (2019) New frontiers in the biosynthesis of metal oxide nanoparticles and their environmental applications: an overview. SN Appl Sci 1(8):928. https://doi.org/10.1007/s42452-019-0931-4

Ghaly MY, Jamil TS, El-Seesy IE, Souaya ER, Nasr RA (2011) Treatment of highly polluted paper mill wastewater by solar photocatalytic oxidation with synthesized nano TiO_2. Chem Eng J 168:446–454. https://doi.org/10.1109/GTEC.2011.6167693

Ghulam N, Qurat-Ul-Ain, Bilal TM, Khalid NR, Tahir I, Muhammad R, Sajad H, Waseem R, Imran A, Muhammad R (2020) Green synthesis of TiO_2 nanoparticles using lemon peel extract: their optical and photocatalytic properties. Int J Environ Anal Chem 0306-7319. https://doi.org/10.1080/03067319.2020.1722816

Jalill RDHA, Nuaman RS, Abd AN (2016) Biological synthesis of titanium dioxide nanoparticles by *Curcuma longa* plant extract and study its biological properties. World Sci News 49:204–222

Jochebed OG, Jacob KA, Fidelis MK (2017) Total phenol content and antioxidant activity of Okra seeds from different genotypes. Am J Food Nutr 5(3):90-94. https://doi.org/10.12691/ajfn-5-3-2

Karakitsou KE, Verykios XE (1993) Effects of altervalent cation doping of TiO_2 on its performance as a photocatalyst for water cleavage. J Phys Chem 97:1184–1189. https://doi.org/10.1021/j100108a014

Khan SU, Al-Shahry M, Ingler WB (2002) Efficient photochemical water splitting by a chemically modified n-TiO_2. Science 297:2243–2245. https://doi.org/10.1126/science.1075035

Kuppusamy P, Yusoff MM, Maniam GP, Govindan N (2016) Biosynthesis of metallic nanoparticles using plant derivatives and their new avenues in pharmacological applications–an updated report. Saudi Pharm J 24:473–484. https://doi.org/10.1016/j.jsps.2014.11.013

Mahshid S, Askari M, Ghamsari MS (2007) Synthesis of TiO_2 nanoparticles by hydrolysis and peptization of titanium isopropoxide solution. J Mater Process Technol 189:296–300. https://doi.org/10.1016/j.jmatprotec.2007.01.040

Makarov VV, Love AJ, Sinitsyna OV, Makarova SS, Yaminsky IV, Taliansky ME, Kalinina NO (2014) "Green" nanotechnologies: synthesis of metal nanoparticles using plants. Acta Nat 6:35–44

Mohamed K, Zine K, Fahima K, Abdelfattah E, Sharifudin SM, Duduku K (2018) NiO nanoparticles induce cytotoxicity mediated through ROS generation and impairing the antioxidant defense in the human lung epithelial cells (A549): Preventive effect of *Pistacia lentiscus* essential oil. Toxicol Rep 5:480–488. https://doi.org/10.1016/j.toxrep.2018.03.012

Mohanpuria P, Rana NK, Yadav SK (2008) Biosynthesis of nanoparticles: technological concepts and future applications. J Nanoparticle Res 10:507–517. https://doi.org/10.1007/s11051-007-9275-x

Moradnia F, Saeid TF, Ali R, Samira O, Ilnaz A (2020) Green sol–gel synthesis of $CoMnCrO_4$ spinel nanoparticles and their photocatalytic application. Micro Nano Lett 15(10):674–677. https://doi.org/10.1049/mnl.2020.0189

Nabi G, Raza W, Tahir MB (2020) Green synthesis of TiO_2 nanoparticle using cinnamon powder extract and the study of optical properties. J Inorg Organomet Polym Mater 30(4):1425–1429. https://doi.org/10.1007/s10904-019-01248-3

Narayanan KB, Sakthivel N (2011) Green synthesis of biogenic metal nanoparticles by terrestrial and aquatic phototrophic and heterotrophic eukaryotes and biocompatible agents. Adv Colloid Interface Sci 169:59–79. https://doi.org/10.1016/j.cis.2011.08.004

Nitin AM, Vitthal SS, Sandip BK, Gurumeet CW, Maryappa CS (2021) Degradation of dyes using biologically synthesized zinc oxide nanoparticles. Mater Today 37:849–853. https://doi.org/10.1016/j.matpr.2020.06.037

Nnamezie AA, Famuwagun AA, Gbadamosi SO (2021) Characterization of okra seed flours, protein concentrate, protein isolate and enzymatic hydrolysates. Food Prod Process and Nutr 14(3):3013–302. https://doi.org/10.1186/s43014-021-00059-9

Paola AD, Garcia-Lopez E, Marci G, Palmisano L (2012) A survey of photocatalytic materials for environmental remediation. J Hazard Mater 212:3–29. https://doi.org/10.1016/j.jhazmat.2011.11.050

Patidar V, Jain P (2017) Green synthesis of TiO_2 nanoparticle using *Moringa oleifera* leaf extract. Int Res J Eng Technol 4:470–473

Peiro AM, Peral J, Domingo C, Momenech X, Ayllon JA (2011) Low-temperature deposition of TiO_2 thin films with photocatalytic activity from colloidal anatase aqueous solutions. Chem Mater 13:2567–2573. https://doi.org/10.1021/cm0012419

Rajabi HR, Khani O, Shamsipur M, Vatanpour V (2013) High performance pure and Fe3+-ion doped ZnS quantum dots as green nano photocatalysts for the removal of malachite green under UV-light irradiation. J Hazard Mater 251:370–378. https://doi.org/10.1016/j.jhazmat.2013.02.007

Ramimoghadam D, Bagheri S, Abd Hamid SB (2014) "Biotemplated synthesis of anatase titanium dioxide nanoparticles via lignocellulosic waste material. Biomed Res Int 205-636https://doi.org/10.1155/2014/205636

Sabouri Z, Akbari A, Hosseini HA, Khatami M, Darroudi M (2020) Egg white-mediated green synthesis of NiO nanoparticles and study of their cytotoxicity and photocatalytic activity. Polyhedron 178:114351. https://doi.org/10.1016/j.poly.2020.114351

Saien J, Ojaghloo Z, Soleymani AR, Rasoulifard MH (2011) Homogeneous and heterogeneous AOPs for rapid degradation of Triton X-100 in aqueous media via UV light, nano titania hydrogen peroxide and potassium persulfate. Chem Eng J 167:172–182. https://doi.org/10.1016/j.cej.2010.12.017

Sandhanasamy D, Mohamad SA (2021) Green synthesis of silver nanoparticles using the flower extract of *Abelmoschus esculentus* for cytotoxicity and antimicrobial studies. Int J Nanomed 16:3343–3356. https://doi.org/10.2147/IJN.S307676

Santhoshkumar T, Rahuman AA, Jayaseelan C, Rajakumar G, Marimuthu S, Kirthi AV, Velayutham K, Thomas J, Venkatesan J, Kim SK (2014) Green synthesis of titanium dioxide nanoparticles using *Psidium guajava* extract and its antibacterial and antioxidant properties. Asian Pac J Trop Med 7(12):968–976. https://doi.org/10.1016/S1995-7645(14)60171-1

Saxena A, Tripathi RM, Zafar F, Singh P (2012) Green synthesis of silver nanoparticles using aqueous solution of *Ficus benghalensis* leaf extract and characterization of their antibacterial activity. Mater Lett 67:91–94. https://doi.org/10.1016/j.matlet.2011.09.038

Surya PG, Gaurav S, Varunika S, Anil KY, Ram NB, Khem BT (2018) Green synthesis of TiO_2 nanoparticles using leaf extract

of *Jatropha curcas L.* for photocatalytic degradation of tannery wastewater. Chem Eng J 336:386–396. https://doi.org/10.1016/j.cej.2017.12.029

Turchi CS, Ollis DF (1990) Photocatalytic degradation of organic water contaminants: mechanisms involving hydroxyl radical attack. J Catal 122:178–192. https://doi.org/10.1016/0021-9517(90)90269-P

Vijayakumar S, Vidhya E, Anand GC, Nilavukkarasi M, Punitha VN, Sakthivel B (2020) Eco friendly synthesis of TiO_2 nanoparticles using aqueous *Ocimum americanum L.* leaf extracts and their antimicrobial, anti-proliferative and photocatalytic activities. Vegetos 33:805–810. https://doi.org/10.1007/s42535-020-00152-3

Waseem A, Krishna KJ, Shivani S (2020) Green synthesis of titanium dioxide (TiO_2) nanoparticles by using *Mentha arvensis* leaves extract and its antimicrobial properties. Inorg Nano-Met Chem 50:1032–1038. https://doi.org/10.1080/24701556.2020.1732419

Xu H, Wang X, Zhang L (2008) Selective preparation of nanorods and micro-octahedrons of Fe_2O_3 and their catalytic performances for thermal decomposition of ammonium perchlorate. Powder Technol 185:176–180. https://doi.org/10.1016/j.powtec.2007.10.011

Zinatizadeh AAL, Mohamed AR, Mashitah MD, Abdullah AZ, Isa MH (2007) Optimization of pretreated palm oil mill digestion in an up-flow anaerobic sludge fixed film bioreactor: a comparative study. Biochem Eng J 35:226–237. https://doi.org/10.1016/j.bej.2007.01.018